



Article

Classification of topological trivial matter with non-trivial defects

Lokman Tsui^a, Zi-Xiang Li^a, Yen-Ta Huang^a, Steven G. Louie^{a,b}, Dung-Hai Lee^{a,b,*}^a Department of Physics, University of California, Berkeley, CA 94720, USA^b Materials Sciences Division, Lawrence Berkeley National Laboratory, Berkeley, CA 94720, USA

ARTICLE INFO

Article history:

Received 9 February 2019

Received in revised form 12 March 2019

Accepted 13 March 2019

Available online 3 April 2019

Keywords:

Majorana zero mode

Symmetry protected topological phase

Topological superconductor

Topological defect

K-theory

ABSTRACT

In this paper, we apply the K-theory to classify topological trivial fermionic phases which, nonetheless, host symmetry-protected non-trivial defects. An important implication of our work is that the existence of Majorana zero mode in the vortex core is neither a necessary nor a sufficient condition for the superconductor in question being topologically non-trivial.

© 2019 Science China Press. Published by Elsevier B.V. and Science China Press. All rights reserved.

1. Introduction

Electronic phases with symmetry protected defect zero modes has attracted tremendous interest in condensed matter physics. Often, the involved fermionic phases possess topological non-trivial electronic structure. A famous example is the pioneer work of Read and Green [1]. They showed that the spin-polarized 2D superconductor with $p_x + ip_y$ pairing symmetry is topological. This is manifested in the existence of chiral boundary Majorana fermions and the Majorana zero mode in the vortex core. Majorana fermion is the antiparticle of itself. A pair of Majorana zero modes produces a twofold degeneracy in the Hilbert space. Because of such degeneracy, and the Berry phase caused by the braiding, Majorana vortices are shown to exhibit non-abelian statistics. Due to this property and the fact that Majorana zero modes are robust against local symmetry-preserving perturbations, they are proposed to be the qubits for topological quantum computing. This possibility makes the Majorana zero mode a focus of many theoretical and experimental studies [2–6].

Lots of experimental efforts have been devoted to searching the Majorana zero modes. For example, Majorana zero mode with quantized tunneling conductance has been observed at the end of superconducting quantum wire [7]. In two space dimensions, evidence for zero-bias peaks in the superconducting vortices has been reported for $\text{Bi}_2\text{Se}_3/\text{NbSe}_2$ [8] and $\text{Fe}(\text{Te}_{1-x}\text{Se}_x)$ [9]. However

whether these zero-bias peaks are due to Majorana zero modes is still under investigation. Theoretically various proposals for realizing Majorana zero modes, e.g., Refs. [2,10,11], have been put forward.

The non-abelian statistics of Majorana vortices makes them highly unusual excitations. In the literature, it is commonly believed that non-abelian anyons can only occur in topologically non-trivial systems. In this paper, we ask the question whether a topologically trivial system can nonetheless support this type of novel excitations.

We enumerate all topologically trivial electronic phases which possess symmetry-protected non-trivial defects. It turns out such possibility requires the spatial dimension, d , to be greater or equal to two. The main result of this work is summarized in Tables 1 and 2, which is derived from Table 1 of Ref. [12], Table 1 of Ref. [13], Table 3 of Ref. [14], and Table 1 of Ref. [15]. We reproduce them as Table SM-I in the Supplementary data (online) for easy reference.

The first column of Tables 1 and 2 is the spatial dimension. The second and third columns give the classification for “codimension” 2 and codimension 3 defects (see the table caption for the definition of codimension). Classification of codimension 1 defects is the same as the bulk classification. Thus the only way for a 1D superconducting wire to exhibit Majorana zero mode at the two ends (which are zero dimension defects and have $k = 1 - 0 = 1$) is for the wire to be topologically non-trivial [10,16–18]. The fourth column gives the bulk classification. The last column specifies the ten-fold-way classes to which the systems belong.

* Corresponding author.

E-mail address: dunghai@berkeley.edu (D.-H. Lee).

Table 1

The classification table for trivial bulk and non-trivial defect. Here d is the spatial dimension and k is the codimension of the defects. The codimension is the difference between the spatial dimension and the dimension of the defects. The classification of codimension 1 defects is the same as the bulk classification hence is not included.

d	$k = 2$	$k = 3$	Bulk	Ten-fold-way class
2	Z	NA	0	BDI
2	Z	NA	0	CII
2	Z	NA	0	AIII
3	0	Z	0	BDI
3	Z	Z_2	0	D
3	Z	0	0	C
3	Z	0	0	A

Table 2

The classification table for non-trivial bulk but trivial defect.

d	$k = 2$	$k = 3$	Bulk	Ten-fold-way class
2	0	NA	Z_2	AII
2	0	NA	Z	C
2	0	NA	Z	A
3	0	0	Z	CI

In the following, we briefly explain how to deduce [Tables 1](#) and [2](#) from Table SM-I (online). Table SM-I is arranged according to the Bott periodicity theorem [19]. Each ten-fold-way class is associated with an integer p which is defined either Mod(8) or Mod(2). To find the bulk classification, one first locates the appropriate ten-fold-way class p from column 4 which lists the generators of symmetry and their commutation relation [14]. For example, if the problem has time reversal ($T^2 = -1$) and charge conservation, the ten-fold-way class is AII or $p = 4$. If the space dimension is d , we move up d rows. Thus for $p = 4$ and $d = 3$, we move to the row labeled as $p = 1$ hence the bulk classification is Z_2 .

Defects are singularities in the free fermion Hamiltonian. For example, a vortex is a point defect in the BdG Hamiltonian of a 2D superconductor. It is important to remember that in finding out the defect classification [15] one needs to specify the Hamiltonian symmetry in the presence of defects. Each defect is characterized by its codimension k . For example a point defect has $k = d$ and a line defect has $k = d - 1 \dots$ etc. To deduce the defect classification we again first locate the ten-fold-way class corresponding to the appropriate symmetry. Then we move up $d - k + 1$ rows. For example for 2D superconductors with an anti-unitary symmetry $T_+^2 = +1$ the ten-fold-way class is BDI or $p = 1$. The classification of vortices ($k = 2$) is given by the third column of the $p = 0$ row, hence the Z classification. This means a vorticity $+n$ vortex will have n Majorana zero modes protected by symmetry.

In the following we provide examples of [Table 1](#), paying special attention to superconductors. According to Table SM-I (online), we conclude that 2D superconductor in the BDI class (i.e. $p = 1$ Mod(8)) is trivial. However as described above, its vortex classification is Z which is non-trivial. Similarly 3D superconductors with no symmetry, i.e., the D class ($p = 2$ Mod(8)) are topologically trivial, however their vortex lines are classified by Z, i.e., a vorticity n vortex line harbors n branches of chiral-dispersing Majorana modes in the vortex core. In the following we provide explicit simple models for the 2D and 3D examples mentioned above.

2. Example in 2D

Here we consider a spin-singlet superconductor with $T_+^2 = +1$ symmetry. In continuum space, the Hamiltonian reads

$$H = \int d^2x \chi^\dagger(\mathbf{x}) (-iZ\partial_1 - iX\partial_2 - i\phi_1XE - i\phi_2ZE) \chi(\mathbf{x}). \quad (1)$$

Here $\chi(\mathbf{x})$ is a four component Majorana fermion operator. The anti-unitary symmetry T_+ is represented by $T_+ = EE$. Here we abbreviate the Kronecker product of Pauli matrices, e.g., $\sigma_0 \otimes \sigma_x$ as IX , etc, and EE denotes $i\sigma_y \otimes i\sigma_y$. Note the first two terms of this Hamiltonian are the same as that describing the surface state of Bi_2Se_3 . With charge conservation and time reversal $T_-^2 = -1$ symmetry such Hamiltonian can not be realized on a two dimensional lattice. However in the presence of the symmetry-breaking “mass” terms ϕ_1 and ϕ_2 , which represent the real and imaginary part of the spin singlet superconducting pair field induced through the proximity effect, this model can be regularized on a 2D lattice [20]. In other words, Eq. (1) can be realized as the low-energy effective Hamiltonian of the lattice model presented below:

$$H = \sum_{k \in \text{BZ}} \chi_{-k}^\dagger [\sin(k_x)IZ + \sin(k_y)IX - (1 - \cos(k_x))iXE - (1 - \cos(k_y))iZE - \phi_1 iXE - \phi_2 iZE] \chi_k, \quad (2)$$

where the third and fourth terms are regularization terms that gap out spurious Dirac points at momentum $(0, \pi)$, $(\pi, 0)$, and (π, π) .

To save space and avoid lengthy equations, in the rest of the paper, we will refer the readers to the SM for all lattice version of the continuum Hamiltonian presented in the main text. However we will summarize the result of calculations made on those lattice Hamiltonians to keep the main text self contained.

To check whether the bulk superconductor given by Eq. (2) is topologically trivial, we diagonalize the real space version of Eq. (2) on a cylinder with periodic (open) boundary condition in the $x(y)$ directions. The result is given in [Fig. 1](#). It shows there is no symmetry-protected gapless edge state, consistent with the statement that the bulk is trivial.

To check whether the vortices harbor Majorana zero modes, we use the following spatial dependence order parameter

$$\phi_1(\mathbf{x}) + i\phi_2(\mathbf{x}) = \Delta_0 \left[\frac{(x - x_0) + i(y - y_0)}{|(x - x_0) + i(y - y_0)|} \frac{(x - x_1) - i(y - y_1)}{|(x - x_1) - i(y - y_1)|} \right]^{n_v}, \quad (3)$$

in the real space version of Eq. (2). Here (x_0, y_0) and (x_1, y_1) are the centers of a pair of $\pm n_v$ vortices. In [Fig. 2a](#) and [b](#), we show the eigen spectra for the case where $n_v = 1$. It shows that there is a pair of Majorana zero modes, one associated with the vortex and the other associated with antivortex, respectively. This result is supplemented by the analytic solution of the Majorana zero mode in a single vortex in Section IV in the [Supplementary data \(online\)](#). In [Fig. 2c](#), we plot the sum of the modulus square of the eigenfunctions associated with the pair of zero modes. It clearly shows that the zero modes are localized in the core of the vortices. According to

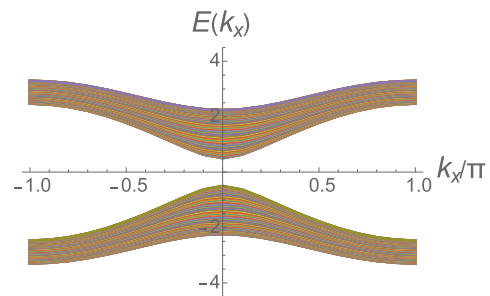


Fig. 1. (Color online) Projected band structure of the real space version of Eq. (2) with periodic boundary condition in \hat{x} and open boundary condition in \hat{y} . The number of rows in y direction, n_y , is 80. The $\phi_{1,2}$ used to generate this plot are $\phi_1 = 0.5 \cos \theta$ and $\phi_2 = 0.5 \sin \theta$, where $\theta = \pi/8$. Since the symmetry is the same for any value of θ , the existence of a θ value for which there is no gapless edge state is sufficient to prove there is no symmetry-protected gapless edge modes.

the analytic solution, the wavefunctions of the Majorana zero modes should be the eigenfunctions of YY with eigenvalue ± 1 (+ for the vortex and – for the anti-vortex). In Fig. 2d we plot the sum of the expectation value of YY in the vortex/antivortex zero modes. The result is consistent with the analytic solution. In addition to the above results, in Fig. 2a, b we compare the energy spectrum of a pair of ± 1 vortices with that of a pair of ± 2 vortices. We see that the number of zero modes has doubled. This is consistent with the classification of the vortex being Z .

But what about a single $n_v = 1$ vortex in a disk? Since Majorana zero mode must appear in pairs, there must be a zero mode on the boundary of the disk. This is indeed the case as shown in Fig. 3. There we consider a cylinder and show that when (ϕ_1, ϕ_2) wind around the azimuthal direction (Fig. 3a), a Majorana zero mode appears on each of the open edges (Fig. 3c and d). By shrinking one of the edge circle to a point to mimic the vortex core, and regard the other circular edge as the boundary of the disk (Fig. 3b), this implies the presence of a Majorana zero mode in the vortex core and on the disk boundary.

We note that other 2D examples of topological trivial states with non-trivial defects are discussed in Refs. [21,22].

3. Example in 3D

According to Table 1 the ten-fold-way class D has a trivial superconductor in 3D with non-trivial vortex lines. It turns out that by adding one gamma matrix to Eq. (1) we can obtain a Hamiltonian describing such a superconductor:

$$H = \int d^3x \chi^\dagger(\mathbf{x}) (-iZ\partial_1 - iIX\partial_2 - iEE\partial_3 - i\phi_1XE - i\phi_2ZE) \chi(\mathbf{x}). \quad (4)$$

In Fig. 4a, we plot the projected bandstructure for a system periodic in \hat{x} and \hat{y} and open in \hat{z} . The absence of gapless boundary modes signifies the topological trivialness of the bulk superconductor. In Fig. 4b, we plot the energy spectrum of a pair of ± 1 vortices with their core line running in the z direction. Here the boundary conditions are open in \hat{x}, \hat{y} and periodic in \hat{z} . A pair of chiral-dispersing gapless Majorana modes are present, with the up/down moving branch localized on the vortex/antivortex, respectively. Again, we have a trivial superconductor harboring non-trivial chiral Majorana modes in the vortex cores!

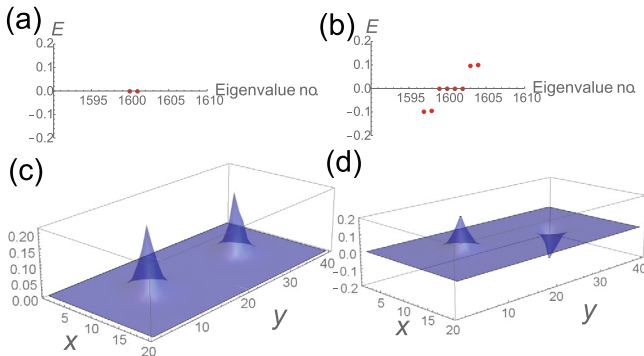


Fig. 2. (Color online) Majorana zero modes in superconducting vortices. (a), (b) The energy spectra of the ± 1 and ± 2 vortex pairs in the lattice model for the $T_+^2 = +1$ superconductor. The results are obtained by setting $\Delta_0 = 0.5$ in Eq. (3). For the ± 1 vortex pair, panel (c) is the sum of the modulus square of the two zero mode wavefunctions. Panel (d) shows $M(\mathbf{x}) = \langle \Phi_1(\mathbf{x}) | YY | \Phi_1(\mathbf{x}) \rangle + \langle \Phi_2(\mathbf{x}) | YY | \Phi_2(\mathbf{x}) \rangle$ where $|\Phi_1(\mathbf{x})\rangle$ and $|\Phi_2(\mathbf{x})\rangle$ are the 4-component eigenfunctions of the two Majorana zero modes. The calculation is done under open boundary condition with 40×20 sites ($40/20$ in the direction parallel/perpendicular to the separation vector between the vortices).

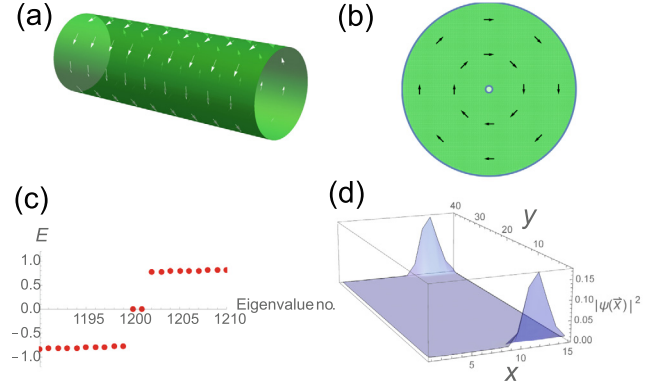


Fig. 3. (Color online) Majorana zero modes in an open cylinder with order parameter winding. (a) A superconductor defined on a cylinder, with the order parameter winding around a non-contractible cycle. (b) A punctured disk with order parameter winding around the center, and along the outer perimeter of the disk. It can be viewed as a deformation of the cylinder in (a). (c) The energy spectra of the real space version of Eq. (2) on a cylinder with order parameter winding in the azimuthal direction. There are two zero modes. (d) The sum of modulus square of the two zero mode eigenfunctions. They are localized on the boundary of the cylinder. Since the order parameter breaks the translation symmetry in the x -direction, the zero mode is not uniformly spread over the circumference of the cylinder.

4. Experimental relevance

Fu and Kane [11] made a novel proposal to realize the Majorana vortices by proximity-inducing superconductivity on the surface of 3D topological insulators. This breaks the charge conservation. In addition, if one applies a magnetic field to induce vortices, the $T_-^2 = -1$ symmetry is also broken. Under this condition the following Hamiltonian describes the surface states

$$H = \int d^2x \chi^\dagger(\mathbf{x}) (-iLZ\partial_1 - iIX\partial_2 - i\phi_1(\mathbf{x})XE - i\phi_2(\mathbf{x})ZE - i\phi_3IE) \chi(\mathbf{x}). \quad (5)$$

Here ϕ_1 and ϕ_2 are the same superconducting order parameter as in Eq. (1). ϕ_3 , on the other hand, is a magnetization order parameter which is permitted due to the breaking of the time reversal symmetry. As one tunes the ratio between ϕ_3 and $\sqrt{\phi_1^2 + \phi_2^2}$ a gap-closing phase transition occurs on the conical surface shown in Fig. 5c. In the phases where ϕ_3 dominates the surface will show quantized Hall conductance with the sign determined by that of ϕ_3 . In the phase where $\sqrt{\phi_1^2 + \phi_2^2}$ dominates the system is a superconductor. Moreover when $\phi_3 = 0$ there is an extra symmetry, namely, the T_+ of Eq. (1). Due to the breaking of the original time reversal and charge conservation symmetries of the 3D topological insulator, these phases can be realized in 2D lattice models [20]. In Section VII of the Supplementary data (online), we present the result of a lattice diagonalization which shows that the interface between the quantized anomalous Hall [23,24] and the superconducting phases possesses chiral Majorana modes [25], consistent with them being inequivalent topological phases. Interestingly, in the presence of non-zero ϕ_3 (but still in the $\sqrt{\phi_1^2 + \phi_2^2}$ dominating phase) the vortex classification becomes Z_2 as shown by the gapped core of double vortices in Fig. 5b, which agrees with the expectation of Fu and Kane [11].

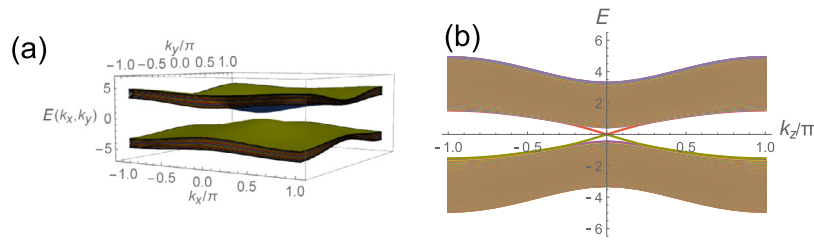


Fig. 4. (Color online) Gapless Majorana modes in vortex core lines in a trivial 3D superconductor. (a) The projected bandstructure of the lattice version of Eq. (4) with periodic boundary condition in \hat{x}, \hat{y} and open boundary condition in \hat{z} . There are $n_z = 40$ planes in the \hat{z} direction. The $\phi_{1,2}$ used to generate this plot are $\phi_1 = 0.5 \cos(\pi/8)$ and $\phi_2 = 0.5 \sin(\pi/8)$. The same reason as that stated in the caption of Fig. 1 implies there are no symmetry-protected surface modes. (b) The spectrum of a pair of ± 1 vortex tubes. The vortex tubes are running in the \hat{z} direction which is subjected to periodic boundary condition, with open boundary conditions in \hat{x} and \hat{y} . In the x - y plane, the number of sites parallel/perpendicular to the vector separating the two vortices are 40/20, respectively. The Δ_0 in Eq. (3) is set to 0.5.

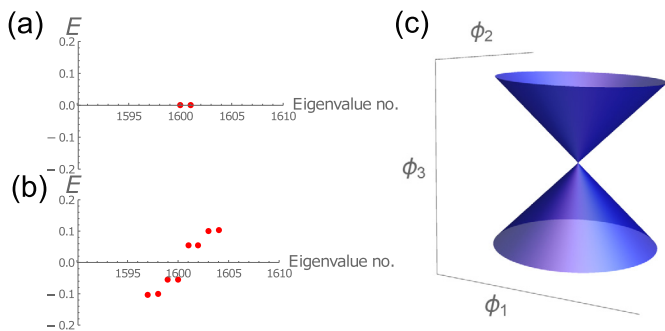


Fig. 5. (Color online) Effect of magnetic order parameter ϕ_3 . (a), (b) The energy spectra of the ± 1 and ± 2 vortex pairs in the presence of a non-zero $\phi_3 = 0.2$. The Δ_0 value is 0.5. The system size is 40×20 sites (40/20 in the direction parallel/perpendicular to the separation vector between the vortices). (c) The surface (blue) of gap closing transition in the space spanned by $\phi_1 - \phi_2 - \phi_3$ in Eq. (5).

5. Discussions and conclusion

So far we have shown that the presence of vortex Majorana modes is not a sufficient condition for concluding the parent superconductor is topologically non-trivial. However is it a necessary condition? The answer is negative as shown by Table 2. For example a 2D superconductor in class All of the ten-fold way has Z_2 bulk classification. However its vortex classification is trivial. Thus zero-mode-possessing defects are neither the sufficient nor the necessary condition for topological non-trivial bulk.

Conflict of interest

The authors declare that they have no conflict of interest.

Acknowledgments

We thank Prof. Fa Wang for useful discussions. This work was supported by the Theory Program at the Lawrence Berkeley National Laboratory, which is funded by the U.S. Department of Energy, Office of Science, Basic Energy Sciences, Materials Sciences and Engineering Division under Contract No. DE-AC02-05CH11231.

Author contributions

D.-H.L. supervised this project. L.T., Z.-X.L, Y.-T.H and D.-H.L. performed the research. L.T., S.G.L and D.-H.L. wrote the paper.

Appendix A. Supplementary data

Supplementary data to this article can be found online at <https://doi.org/10.1016/j.scib.2019.04.006>.

References

- [1] Read N, Green D. Symmetry protected topological Luttinger liquids and the phase transition between them. *Phys Rev B* 2000;61:10267.
- [2] Alicea J. New directions in the pursuit of Majorana fermions in solid state systems. *Rep Prog Phys* 2012;75:076501.
- [3] Elliott SR, Franz M. Colloquium: majorana fermions in nuclear, particle, and solid-state physics. *Rev Mod Phys* 2015;87:137.
- [4] Sato M, Ando Y. Topological superconductors: a review. *Rep Prog Phys* 2017;80:076501.
- [5] Aguado R. Majorana quasiparticles in condensed matter. *Riv Nuovo Cimento* 2017;40:523.
- [6] Lutchyn RM, Bakkers E, Kouwenhoven LP, et al. Majorana zero modes in superconductor semiconductor heterostructures. *Nat Rev Mater* 2018;3:52–68.
- [7] Mourik V, Zuo K, Frolov SM, et al. Signatures of Majorana fermions in hybrid superconductor-semiconductor nanowire devices. *Science* 2012;336:1003–7.
- [8] Sun HH, Zhang KW, Hu LH, et al. Majorana zero mode detected with spin selective Andreev reflection in the vortex of a topological superconductor. *Phys Rev Lett* 2016;116:257003.
- [9] Zhang P, Yaji K, Hashimoto T, et al. Observation of topological superconductivity on the surface of an iron-based superconductor. *Science* 2018;360:182–6.
- [10] Lutchyn RM, Sau JD, Das Sarma S. Majorana fermions and a topological phase transition in semiconductor-superconductor heterostructures. *Phys Rev Lett* 2010;105:077001.
- [11] Fu L, Kane CL. Superconducting proximity effect and Majorana fermions at the surface of a topological insulator. *Phys Rev Lett* 2008;100:096407.
- [12] Schnyder AP, Ryu S, Furusaki A, et al. Classification of topological insulators and superconductors in three spatial dimensions. *Phys Rev B* 2008;78:195125.
- [13] Kitaev A. Periodic table for topological insulators and superconductors. *AIP Conf Proc* 2009;1134:20.
- [14] Wen X-G. Symmetry-protected topological phases in noninteracting fermion systems. *Phys Rev B* 2012;85:085103.
- [15] Teo JCY, Kane CL. Topological defects and gapless modes in insulators and superconductors. *Phys Rev B* 2010;82:115120.
- [16] Zhang H, Liu CX, Gazibegovic S, et al. Quantized majorana conductance. *Nature* 2018;556:74–9.
- [17] Kitaev A. Unpaired Majorana fermions in quantum wires. *Phys USP* 2001;44:131.
- [18] Oreg Y, Refael G, von Oppen F. Helical liquids and Majorana bound states in quantum wires. *Phys Rev Lett* 2010;105:177002.
- [19] Bott R. The stable homotopy of the classical groups. *Ann Math* 1959;70:313.
- [20] Qi X-L, Zhang S-C. Topological insulators and superconductors. *Rev Mod Phys* 2011;83:1057.
- [21] Yan Z, Bi R, Wang Z. Majorana zero modes protected by a hopf invariant in topologically trivial superconductors. *Phys Rev Lett* 2017;118:147003.
- [22] Chan C, Zhang L, Poon TFJ, et al. Generic theory for Majorana zero modes in 2D superconductors. *Phys Rev Lett* 2017;119:047001.
- [23] Yu R, Zhang W, Zhang HJ, et al. Quantized anomalous Hall effect in magnetic topological insulators. *Science* 2010;329:61–4.
- [24] Chang CZ, Zhang J, Feng X, et al. Experimental observation of the quantum anomalous Hall effect in a magnetic topological insulator. *Science* 2013;340:167–70.
- [25] Qi X-L, Hughes TL, Zhang S-C. Chiral topological superconductor from the quantum Hall state. *Phys Rev B* 2010;82:184516.



Lokman Tsui is a graduate from the Hong Kong University of Science and Technology in 2008 and obtained his master degree from Perimeter Scholars International Program in 2010. He finished his doctoral degree in University of California, Berkeley in 2018. He is currently a postdoctoral fellow in Massachusetts Institute of Technology and he is broadly interested in topological phases, their protected surfaces and their critical phenomena.



Dung-Hai Lee received his B.S. degree from the Tsinghua University of Taiwan. He went to the Massachusetts Institute of Technology in 1977 for graduate studies, and received his Ph.D. degree in physics in 1982. After staying at M.I.T. for another two years, he joined the IBM T.J. Watson Research Center in 1984. He spent 11 years at IBM, and went to Berkeley in February 1994. The principal goal of his research is to uncover new states of matter and understand their physical properties. His current interest is in the physics of novel superconductors and topological states in condensed matter systems.